

Synthesis and hyperthermia property of hydroxyapatite-ferrite hybrid particles by ultrasonic spray pyrolysis

Akihiro Inukai ^a, Naonori Sakamoto ^a, Hiromichi Aono ^b, Osamu Sakurai ^c, Kazuo Shinozaki ^c, Hisao Suzuki ^d, and Naoki Wakiya ^a

^a Department of Materials Science and Chemical Engineering, Shizuoka University, 3-5-1 Johoku Naka-ku, Hamamatsu 432-8561, Shizuoka Japan

^b Materials Science and Biotechnology, Graduate School of Science and Engineering, Ehime University, 3 Bunkyo-cho, Matsuyama, 790-8577 Japan

^c Department of Metallurgy and Ceramics Science, Tokyo Institute of Technology, 2-12-1 O-okayama Meguro-ku, Tokyo 152-8550, Japan

^d Graduate School of Materials Science and Technology, Shizuoka University, 3-5-1 Johoku Naka-ku, Hamamatsu 432-8561, Shizuoka Japan

Corresponding author. Tel./fax: +8153 4781153.

E-mail: tnwakiy@ipc.shizuoka.ac.jp (N. Wakiya)

Abstract

Biocompatible hybrid particles composed of hydroxyapatite ($\text{Ca}_{10}(\text{PO}_4)_6(\text{OH})_2$, HAp) and ferrite ($\gamma\text{-Fe}_2\text{O}_3$ and Fe_3O_4) were synthesized using a two-step procedure. First, the ferrite particles were synthesized by c-precipitation. Second, the suspension, which was composed of ferrite particles by a coprecipitation method, $\text{Ca}(\text{NO}_3)_2$, and H_3PO_4 aqueous solution with surfactant, was nebulized into mist ultrasonically. Then the mist was

pyrolyzed at 1000°C to synthesize HAp-ferrite hybrid particles. The molar ratio of Fe ion and HAp was $(\text{Fe}^{2+} \text{ and } \text{Fe}^{3+})/\text{HAp} = 6$. The synthesized hybrid particle was round and dimpled, and the average diameter of a secondary particle was 740 nm. The cross section of the synthesized hybrid particles revealed two phases: HAp and ferrite. The ferrite was coated with HAp. The synthesized hybrid particles show saturation magnetization of 11.8 emu/g. The net saturation magnetization of the ferrite component was calculated as 32.5 emu/g. The temperature increase in the ac-magnetic field (370 kHz, 1.77 kA/m) was 9°C with 3.4 g (the ferrite component was 1.0 g). These results show that synthesized hybrid particles are biocompatible and might be useful for magnetic transport and hyperthermia studies.

Keywords

Maghemite, Hydroxyapatite, Hybrid, Core-shell structure, Biocompatible, Hyperthermia

1. Introduction

Ferrite nanoparticles, including magnetite (Fe_3O_4) and its oxidized form, maghemite ($\gamma\text{-Fe}_2\text{O}_3$), are used for many biomedical applications such as media for biosensors [1], magnetic resonance imaging (MRI) [2], immunoassay [3], hyperthermia [4], and drug-delivery systems (DDSs) [5,6]. Hyperthermia, one modality of malignant cancer treatment, currently receives considerable attention. The hyperthermia technique, which advances cancer cell necrosis through the elevation of cell temperature to around 43°C, was introduced recently. Particularly, magnetic fluid hyperthermia (MFH) induced by heating effects in an ac-magnetic field of the magnetic nanoparticles has attracted much

attention because of its safe treatment with little physical or mental strain to the patient. Ferrite nanoparticles have been examined as heat carriers for use in MFH: Fe_3O_4 , $\gamma\text{-Fe}_2\text{O}_3$ [7,8], Co-ferrite (CoFe_2O_4) [9], Mg-ferrite (MgFe_2O_4) [10], etc. However, their application as heat carriers remains subject to limited biocompatibility because the ferrite nanoparticles must be introduced into the blood vessels. Therefore, ferrite nanoparticle surfaces have been coated to date with biocompatible materials such as gold (Au) [11], polymer, silica (SiO_2) [12], titania (TiO_2) [13], and hydroxyapatite ($\text{Ca}_{10}(\text{PO}_4)_6(\text{OH})_2$, HAp) [14]. Among these, HAp-coated ferrite nanoparticles are a most promising material. In its natural state, HAp is the material component of bone. Many studies have examined HAp fabrication [15,16]. Previously, we reported the synthesized of HAp-ferrite composite particles [17]. However, it has a very low magnetic property (saturation magnetization is 0.833 emu/g). Additionally, it is uncertain whether the ferrite nanoparticles are coated with HAp. Therefore, it is difficult to use them as MFH. For that reason, it is necessary to improve their magnetic properties and observe the cross sectional structure of synthesized hybrid particles.

This work was undertaken to synthesize HAp-ferrite hybrid particles with higher magnetization than previously reported, to observe the cross sectional structure of synthesized hybrid particles, and to examine the behavior against application of the AC-magnetic field.

2. Experimental

All chemicals used in the experiments were of analytical reagent grade. Ferrite particles were synthesized by co-precipitation. The $\text{FeSO}_4 \cdot 7\text{H}_2\text{O}$ and $\text{FeCl}_3 \cdot 6\text{H}_2\text{O}$ were weighed and dissolved in the 200 ml deionization water. Though stoichiometric

composition of Fe_3O_4 is $x=33.3$ in $x\text{FeSO}_4-(100-x)\text{FeCl}_3$ in molar ratio, we used $x=40$ in this work due to following reasons;

(1) In our previous work [17], it was found that considerable amount of $\alpha\text{-FeOOH}$ was coexisted with Fe_3O_4 and $\gamma\text{-Fe}_2\text{O}_3$ in the case of $x=33.3$. It was also found that the amount of Fe_3O_4 and $\gamma\text{-Fe}_2\text{O}_3$ was increased and that of $\alpha\text{-FeOOH}$ was decreased with x . Since Fe^{2+} is apt to be oxidized into Fe^{3+} slowly in air, the ratio of $\text{Fe}^{2+}/\text{Fe}^{3+}$ should be increased to compensate the decrease of Fe^{2+} .

(2) In our another previous work[18], it was found that $\alpha\text{-FeOOH}$ enhances the adhesion of HAp.

That is, the starting composition ($x=40$) is selected to achieve a compromise between magnetic ferrites for hyperthermia purpose and antimagnetic $\alpha\text{-FeOOH}$ for adhesion purpose.

To carry out co-precipitation, 100 ml NaOH aqueous solution (1 mol/l) was dropped slowly at the dropping rate of 3 ml/min. After co-precipitation, the supernatant solution was removed, and deionization water was added to wash the sediment. Then the sediment was separated centrifugally. This washing procedure was repeated five times. The sediment was then poured in the deionization water with 0.02 mol/l cetyltrimethyl ammonium bromide (CTAB) surfactant to prepare suspension because Liu et al. reported the validity of CTAB addition to prepare suspension of maghemite ($\gamma\text{-Fe}_2\text{O}_3$) [19]. The suspension (100 ml) was homogenized ultrasonically for 8 h using an ultrasonic homogenizer. Then the suspension (100 ml) was mixed with the 0.5 mol/l HAp source solution (100 ml). Thereby, a precursor for ultrasonic spray pyrolysis was prepared where the HAp source solution consisted of $\text{Ca}(\text{NO}_3)_2 \cdot 4\text{H}_2\text{O}$ and H_3PO_4 . The molar ratio of Fe ion and HAp was $(\text{Fe}^{2+} \text{ and } \text{Fe}^{3+})/\text{HAp} = 6$. Prior to ultrasonic spray pyrolysis, the

precursor was homogenized ultrasonically for another 8 h. Then the precursor was nebulized using 1.6 MHz ultrasonic nebulizer. The generated aerosol was transported by N₂ carrier gas (3 l/min) into a furnace for drying at 100°C followed by heating in a furnace for decomposition at 1000°C. After the decomposition, the particles were collected using a filter.

Crystal structures of the samples was examined using an X-ray diffractometer equipped with a Cu anode (D8 Advance; Bruker Analytik) and phase composition was analyzed using TOPAS software [20]. The magnetic property of the samples was examined using vibration sample magnetometer (VSM)(BHV-35; Riken Denshi Co. Ltd.) measured at room temperature with maximum magnetic field of 10 kOe and frequency of 25 Hz. The magnetization was calibrated using a standard sample of Ni foil. The composition of the hybrid particles was measured using an inductively coupled plasma atomic emission spectrometer (ICP–AES) (Optima 2100DV; PerkinElmer Inc.). Prior to ICP–AES measurement, the particles were dissolved in hydrochloric acid. The microstructure of samples was observed using scanning electron microscopy (SEM) (JSM-5510SV; JEOL) and scanning transmission electron microscopy (STEM) (JEM-2100F; JEOL). To observe the cross sectional microstructure, a thin sheet of particles was fabricated using an ion slicer (EM-09100IS; JEOL). The composition of the individual hybrid particle was measured using energy dispersive x-ray spectroscopy (EDS). The particle size distribution of hybrid particles was measured using an electrophoretic scattering photometer (Photal SELS-800Y; Otsuka Electronics Co. Ltd.). Specific surface areas of powders were measured using BET analysis with nitrogen gas adsorption [21]. Figure 1 depicts the apparatus used for the measurement of the temperature increase in the AC-magnetic field. The powder sample (3.4 g (the ferrite

component was 1.0 g)) was placed in a glass case (Pyrex: 20 mm ϕ , 45 mm). The AC-magnetic field was applied to the sample using an external coil. The coil consisted of loops of copper tubing (6 mm ϕ) around a polypropylene (PP) bobbin (48 mm ϕ \times 40 mm). The copper tube was cooled by flowing water to maintain its impedance. The coil was connected to a power supply (T162-5712B; Thamway Corp.) through an impedance tuner. The output power of 140 W at 370 kHz corresponds to 1.77 kA/m around the center of the coil. An infrared thermometer (505 s; Minolta Co. Ltd.) was used to measure the sample temperature.

3. Results and discussion

The suspension containing the ferrite particles (synthesized by co-precipitation), CTAB, Ca(NO₃)₂•4H₂O and H₃PO₄ was spray-pyrolyzed ultrasonically at 1000°C; the sample was collected. Figure 2 presents XRD patterns of the resultant particles. This figure shows that predominant phases are HAp and ferrite (Fe₃O₄ and γ -Fe₂O₃); a small amount of goethite (α -FeOOH) was also detected. This result indicates that HAp-ferrite hybrid particles are synthesized using ultrasonic spray pyrolysis. Since the X-ray diffraction pattern of Fe₃O₄ and γ -Fe₂O₃ is very similar, we used TOPAS software to distinguish and quantify the amounts of these phases. In addition, the respective amounts of HAp and α -FeOOH were also determined using the software (Table 1). The chemical composition of the hybrid particles was analyzed using ICP–AES (Table 2).

Table 1 shows that the mass fraction of ferrite and HAp is about ferrite/HAp = 2/3, and that the amount of impurity phase (α -FeOOH) is 4.03 wt%. It should be noted that the ferrite is the mixture of Fe₃O₄ and γ -Fe₂O₃ instead of single phase. Since the diameter of primary particles of Fe₃O₄ synthesized by co-precipitation was around 13 nm, most of

Fe_3O_4 were oxidized to form $\gamma\text{-Fe}_2\text{O}_3$ in air even at room temperature. From the point of magnetic property, the saturation magnetization (Ms) of bulk Fe_3O_4 and $\gamma\text{-Fe}_2\text{O}_3$ is 92.1 and 82.4 emu/g, respectively. This indicates that the use of Fe_3O_4 is preferable. However, $\gamma\text{-Fe}_2\text{O}_3$ also has high Ms and high chemical stability, hence we used the mixture of Fe_3O_4 and $\gamma\text{-Fe}_2\text{O}_3$. As mentioned above, molar ratio of Fe ion and HAp was $(\text{Fe}^{2+}$ and $\text{Fe}^{3+})/\text{HAp} = 6$. Therefore, prescribed composition of Ca:P:Fe is calculated to be 45.7:27.3:27.3 mol% as shown in Table 2. The composition of the hybrid particles was measured by ICP-AES. The composition of hybrid particles was also calculated on the basis of TOPAS result. These analytical compositions were also shown in Table 2. The results shown in this table suggests that analytical compositions are in good agreement with prescribed composition within the analytical error. This table also clarifies that the analytical molar rate of Ca/P=1.85 is slightly larger than that of source solution of stoichiometric HAp (Ca/P=1.67). This result suggests that obtained HAp is not the right formula. However, we think that this deviation is also due to the analytical error.

Figure 3 shows an SEM micrograph of HAp-ferrite hybrid particles. This figure indicates that the hybrid particles are round with some dimples, which is characteristic for particles synthesized using spray pyrolysis. The dimple is a feature of the particle synthesized by ultrasonic spray pyrolysis. In the aqueous solution, the dimples on the particles are formed by surface precipitation because of the rapid drying rate of aerosol in the severe preparation condition [22]. But there is a possibility that the dimples on the hybrid particles indicate uncovered surfaces or loosely agglomerated grains. This figure also shows that the size of secondary particle of synthesized hybrid particles varies.

Figure 4 shows the size distribution of secondary particle measured using an electrophoretic scattering photometer. This figure depicts that the size of secondary

particle was between 500–1000 nm with average diameter of 740 nm. The precursor is generated by an ultrasonic nebulizer at 1.6 MHz as the precursor drops. The drop diameters are 4–8 μm with 6 μm peak diameter [23]. Therefore, the product particles were synthesized to uniform size of a nearly microsphere structure.

Figure 5 shows STEM–EDS micrographs of the cross-sectional structure of the hybrid particles: (a) is a STEM image; (b) and (c) respectively show elemental mappings of Ca $K\alpha$ and Fe $K\alpha$. This result shows that a cross section structure of synthesized hybrid particles has two phases (HAp and ferrite) and that ferrite was coated with HAp: the hybrid particles have a core–shell structure composed of a ferrite core and a HAp shell. Therefore, we inferred the generation process of core–shell hybrid particles as follows. The precursor drops generated by an ultrasonic nebulizer contain ferrite particles, which are clumped together in a drop. Furthermore, HAp generates it to surroundings of ferrite particles. Figure 5 also shows that hybrid particles formed a porous morphology. The BET specific surface area of the hybrid particles was 21.2 m^2/g , whereas that of commercial products (HAp; Wako Pure Chemical Industries Ltd.) was 9.11 m^2/g . This result demonstrates that the specific surface area of hybrid particles is higher than that of HAp. The possibility exists that hybrid particles are useful in DDS applications. Actually, HAp have been used in DDS applications [24, 25]. Moreover, HAp with high specific surface area can adsorb large amounts of drugs [26]. Therefore, hybrid particles present the possibility of being an excellent drug carrier. Now we are trying to measure the adsorption and desorption of various drugs.

The magnetic property of the synthesized hybrid particles was measured using VSM at room temperature. Figure 6 shows the M–H curve of the HAp-ferrite hybrid particles. In this figure, magnetization was calculated using the total weight of the sample including

HAp and ferrite. This figure depicts that the saturation magnetization (M_s) of hybrid particles is 11.8 emu/g. Hybrid particles contain the ferrite component by 36.4 wt%. Consequently, we inferred that 36.4% of the mass of the hybrid particle is ferrite. To estimate the state of ferrite, the M–H curve calculated based on the result of TOPAS is depicted in Fig. 7. This figure shows that the estimated net M_s is 32.5 emu/g, which is less than the bulk M_s of 82.4 emu/g for γ -Fe₂O₃ [27], 92.1 emu/g for Fe₃O₄ [28], and 44.3 emu/g for that synthesized by co-precipitation [29]. The lower magnetization than that of the bulk material suggests that crystalline contents are low. In addition, the lower magnetization than that of the co-precipitate suggests that diffusion of Ca into the spinel structure occurred during the spray pyrolysis process because this process is a reaction between the solution and nanoparticles. To consider the diffusion of Ca into a spinel structure, the lattice parameter of γ -Fe₂O₃ in the HAp-ferrite hybrid was calculated as $a=0.8374$ nm. This value is slightly larger than that of pure γ -Fe₂O₃ ($a=0.8352$ nm), suggesting the diffusion of Ca into a spinel structure because the ionic radius of Ca²⁺ (0.100 nm in six-fold coordination) is larger than that of Fe²⁺ (0.078 nm in six-fold coordination). In fact, Fe²⁺ is a magnetic ion, but Ca²⁺ is a nonmagnetic ion. Therefore, net M_s of the ferrite component was lower than that of the co-precipitate. The lowering of magnetization by the use of Ca instead of Fe has been reported by Park et al. [30].

Regarding diffusion, we also consider the possibility of substitution of Ca²⁺ with Fe²⁺ in HAp. The lattice parameters of HAp in the HAp–ferrite hybrid are $a=0.9400$ nm and $c=0.6906$ nm (cell volume of 1.585 nm³). On the other hand, the lattice parameters of pure HAp have been reported as $a=0.9424$ nm and $c=0.6879$ nm (cell volume of 1.587 nm³). The fact that the lattice parameters differ slightly suggests partial substitution. However, the amount of substitution is almost negligible: the cell volume of HAp is

almost unchanged.

Figure 8 shows a typical result for the hyperthermia property in the AC-magnetic field (370 kHz, 1.77 kA/m) for the powder sample (3.4 g; weight of the ferrite component was 1.0 g) of HAp-ferrite hybrid particles. The temperature increase of the sample was measured upon application of the AC-magnetic field over a period of time until it stabilized. The temperature increased and reached almost a steady value after 20 min. For hybrid particles, the increased temperature (ΔT) from room temperature was about 9°C. The specific power absorption rate (SAR) was calculated using the equation given below [31–35].

$$\text{SAR} = \frac{(c_{\text{HAp}} \cdot m_{\text{HAp}} + c_{\text{Fe}_3\text{O}_4} \cdot m_{\text{Fe}_3\text{O}_4} + c_{\gamma\text{-Fe}_2\text{O}_3} \cdot m_{\gamma\text{-Fe}_2\text{O}_3} + c_{\alpha\text{-FeOOH}} \cdot m_{\alpha\text{-FeOOH}}) \cdot \frac{\Delta T}{\Delta t}}{(m_{\text{Fe}_3\text{O}_4} + m_{\gamma\text{-Fe}_2\text{O}_3})}$$

In this equation, c_{HAp} , $c_{\text{Fe}_3\text{O}_4}$, $c_{\gamma\text{-Fe}_2\text{O}_3}$ and $c_{\alpha\text{-FeOOH}}$ represents the specific heat of HAp, Fe_3O_4 , $\gamma\text{-Fe}_2\text{O}_3$ and $\alpha\text{-FeOOH}$, respectively. In a similar way, m_{HAp} , $m_{\text{Fe}_3\text{O}_4}$, $m_{\gamma\text{-Fe}_2\text{O}_3}$ and $m_{\alpha\text{-FeOOH}}$ is the mass of HAp, Fe_3O_4 , $\gamma\text{-Fe}_2\text{O}_3$ and $\alpha\text{-FeOOH}$, respectively. $\Delta T/\Delta t$ stands for the temperature increment rate. For the calculations, the specific heat values of HAp, Fe_3O_4 , $\gamma\text{-Fe}_2\text{O}_3$ and $\alpha\text{-FeOOH}$ were assumed as 1.59, 0.937, 0.75 and 0.78 $\text{JK}^{-1}\text{g}^{-1}$, respectively. The temperature increment rate ($\Delta T/\Delta t$) was evaluated from the temperature-time curve obtained for a measurement time of 60s.

The SAR value of the hybrid particles calculated was 0.0969 W/g. On the other hand, the hysteresis loss of hybrid particles was 0.1247 W/g. The result of comparing SAR with hysteresis loss reaches an almost identical value. Therefore, the heat property in an applied AC-magnetic field depended on the hysteresis loss for the system, except for hybrid particles.

These results suggest that a synthesized HAp-ferrite hybrid particle by ultrasonic spray pyrolysis is biocompatible and has the potential of magnetic transport and hyperthermia.

4. Conclusion

We synthesized HAp–ferrite hybrid particles using two-step synthesis. The first step is synthesis of ferrite particles by co-precipitation of Fe^{2+} and Fe^{3+} aqueous solutions. The ferrite was composed mainly of maghemite ($\gamma\text{-Fe}_2\text{O}_3$) and magnetite (Fe_3O_4). The second step is synthesis of HAp–ferrite hybrid particles using ultrasonic spray pyrolysis at 1000°C using a suspension composed of ferrite particles and $\text{Ca}(\text{NO}_3)_2$ and H_3PO_4 . Formation of HAp–ferrite hybrid was confirmed by X-ray diffraction, composition analysis, cross sectional structure observation, magnetic property measurements, and hyperthermia property measurements. The cross-sectional structure of synthesized hybrid particles showed two phases (HAp and ferrite). The ferrite was coated with HAp. The saturation magnetization of ferrite in the HAp–ferrite hybrid was 32.5 emu/g. The values of saturation magnetization suggest that partial substitution of Ca would occur in the ferrite. The increased temperature in the AC-magnetic field (370 kHz, 1.77 kA/m) was 9°C with 3.4 g (the ferrite component was 1.0 g). Results show that the hybrid particle is biocompatible and that it might be useful for magnetic transport and hyperthermia studies.

References

- [1] H. Chiriac, D.D. Herea, S. Corodeanu, J. Magn. Mater. 311 (2007)

425–428.

- [2] M. Hamoudeh, H. Fessi, *J. Colloid Interface Sci.* 300 (2006) 584–590.
- [3] J.W. Choi, C.H. Ahn, S. Bhansali, H.T. Henderson, *Sens. Actuators B: Chem.* 68 (2000) 34–39.
- [4] R. Hiergeist, W. Andrak, N. Buske, R. Hergt, I. Hilger, U. Richter, W. Kaiser, *J. Magn. Magn. Mater.* 201 (1999) 420–423.
- [5] S. Dandamudi, R.B. Campbell, *Biomaterials* 28 (2007) 4673–4683.
- [6] W. Zheng, F. Gao, H. Gu, *J. Magn. Magn. Mater.* 288 (2005) 403–410.
- [7] M. Kawashita, M. Tanaka, T. Kokubo, Y. Inoue, T. Yao, S. Hamada, T. Shinjo, *Biomaterials* 26 (2005) 2231–2238.
- [8] D.-L. Zhao, X.-W. Zeng, Q.-S. Xia, J.-T. Tang, *J. Alloys Compounds* 469 (2009) 215–218.
- [9] A. Skumiel, *J. Magn. Magn. Mater.* 307 (2006) 85–90.
- [10] H. Hirazawa, S. Kusamoto, H. Aono, T. Naohara, K. Mori, Y. Hattori, T. Maehara, Y. Watanabe, *J. Alloys Compounds* 461 (2008) 467–473.
- [11] H.L. Liu, C.H. Sonn, J.H. Wu, K.-M. Lee, Y.K. Kim, *Biomaterials* 29 (2008) 4003–4011.
- [12] Y. Sun, L. Duan, Z. Guo, Y. DuanMu, M. Ma, L. Xu, Y. Zhang, N. Gu, *J. Magn. Magn. Mater.* 285 (2005) 65–70.
- [13] Y.S. Chung, S.B. Park, D.W. Kang, *Mater. Chem. Phys.* 86 (2004) 375–381.
- [14] N. Petchsang, W. Pon-On, J.H. Hodak, I.M. Tang, *J. Magn. Magn. Mater.* 321 (2009) 1990–1995.
- [15] C. Santos, C.F. Rovath, R.-P. Franke, M.M. Almeida, M.E.V. Costa,

Ceramics International 35 (2009) 509–513.

- [16] S. Bodhak, S. Bose, A. Bandyopadhyay, *Acta Biomaterialia* 6 (2010) 641–651.
- [17] N. Wakiya, M. Yamasaki, T. Adachi, A. Inukai, N. Sakamoto, D. Fu, O. Sakurai, K. Shinozaki, H. Suzuki, *Mater. Sci. Eng. B* 173 (2010) 195–198.
- [18] N. Wakiya, N. Sakamoto, H. Suzuki, T. Ikoma, K. Muraoka, T. Yoshioka, J. Tanaka, O. Sakurai, K. Shinozaki, *Materials Integration* Vol.20 No.11(2007) 44–48 (in Japanese)
- [19] T. Liu, L. Guo, Y. Tao, *Nano Structured Mater.* 11 (1999) 487–492.
- [20] A.A. Coelho, *J. Appl. Cryst.* 33 (2000) 899–908.
- [21] C. Papelis, W. Um, C.E. Russell, Jenny B. Chapman, *Colloids and Surfaces A: Physicochem. Eng. Aspects* 215 (2003) 221–239.
- [22] H. S. Kang, Y. C. Kang, H. D. Park, Y. G. Shul, *Materials Letters* 57 (2003) 1288–1294
- [23] C.Y. Chen, T.K. Tssemg, S.C. Tsai, C.K. Lin, H.M. Lin, *Ceramics International* 34 (2008) 409–416.
- [24] M. Itokazu, T. Sugiyama, T. Ohno, E. Wada, Y. Katagiri, *J. Biomed. Mater. Res.* 39 (1998) 536–538.
- [25] W. Paul, C.P. Sharma, *J. Biomater. Appl.* 17 (2003) 253–264.
- [26] C. Santos, M.A. Martins, R.-P. Franke, M.M. Almeida, M. E. V. Costa / *Ceramics International* 35 (2009) 1587–1594.
- [27] R. Hergt, R. Hiergeist, M. Zeisberger, G. Glockl, W. Weitscies, L.P. Ramirez, I. Hilger, W.A. Kaiser, *J. Magn. Mater.* 280 (2004) 358–368.

- [28] R.J. Kennedy, P.A. Stampe, *J. Phys. D: Appl. Phys.* 32 (1999) 16–21.
- [29] F. Yazdani, M. Edrissi, *Mater. Sci. Eng. B* (2010).
- [30] S.I. Park, J.H. Lim, Y.H. Hwang, J.H. Kim, C.G. Kim, C.O. Kim, *phys. stat. sol.* 204 (2007) 3913–3917.
- [31] L.-Y. Zhang, H.-C. Gu, X.-M. Wang, *J. Magn. Magn. Mater.* 311 (2007) 228–233.
- [32] M. Gonzales-Weimuller, M. Zeisberger, K.M. Krishnan, *J. Magn. Magn. Mater.* 321 (2009) 1947–1950.
- [33] M. Suto, Y. Hirota, H. Mamiya, A. Fujita, R. Kasuya, K. Tohiji, B. Jeyadevan, *J. Magn. Mater.* 321 (2009) 1493–1496.
- [34] P.H. Linh, P.V. Thach, N.A. Tuan, N.C. Thuan, D.H. Manh, N.X. Phuc, L.V. Hong, *J. Phys: Conference Series.* 187 (2009) 012069.
- [35] Z. Li, M Kawashita, N. Araki, M. Mitsumori, M. Hiraoka, M. Doi, *Mater. Sci. Eng. C* 30 (2010) 990-996.

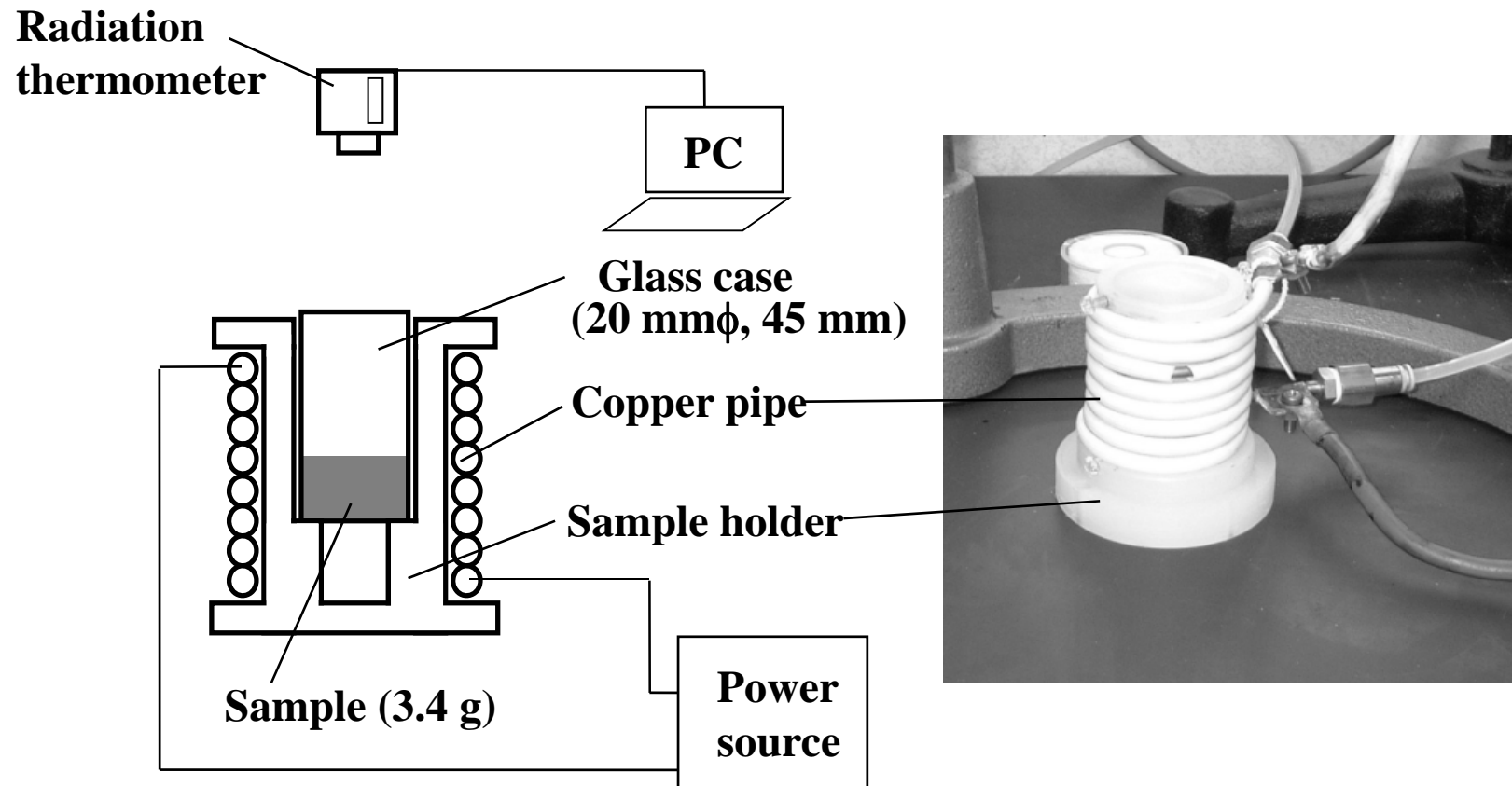


Fig. 1. Apparatus for measuring the heat generation ability of hybrid particles (3.4 g) in an AC-magnetic field (370 kHz, 1.77 kA/m).

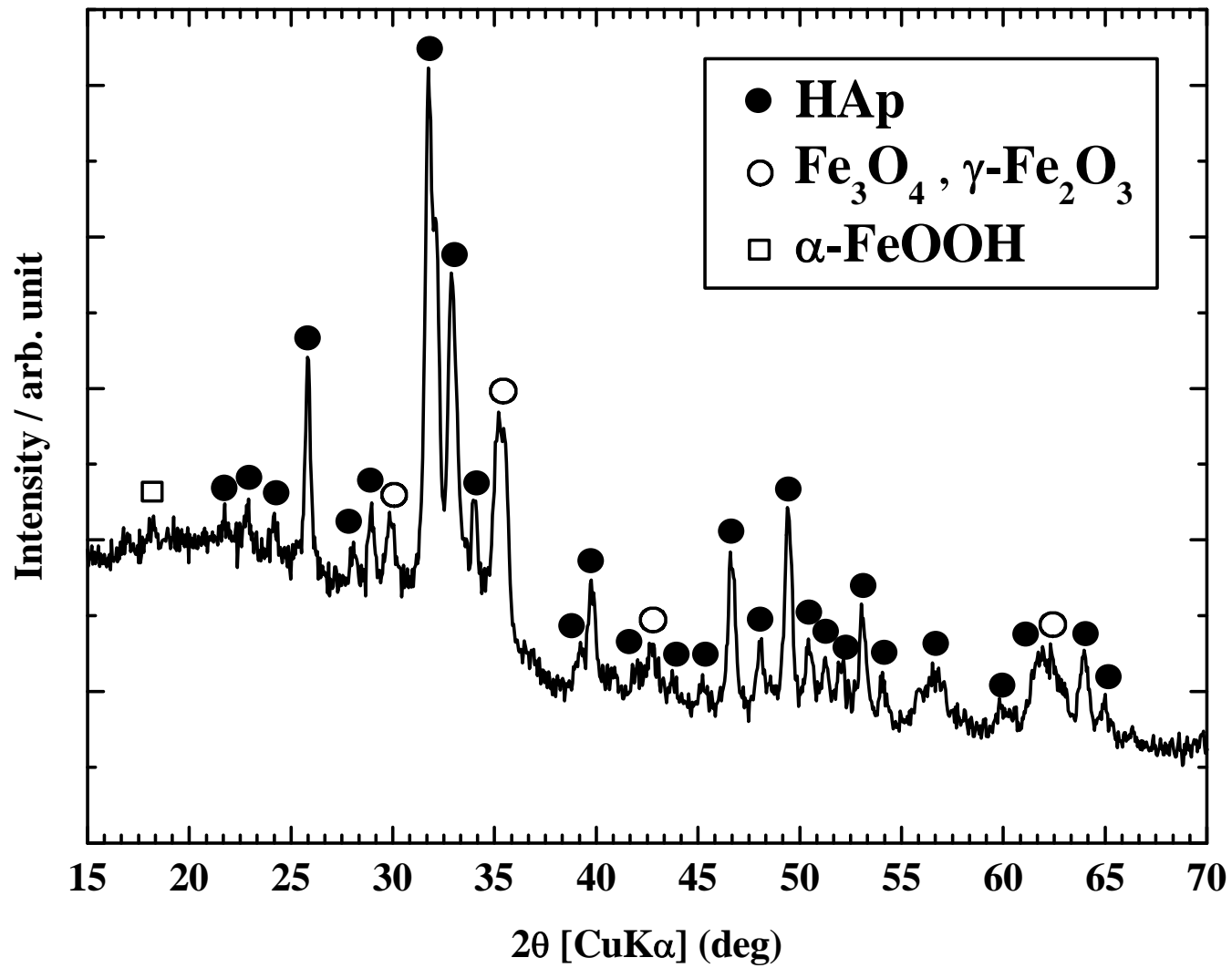


Fig. 2. XRD pattern of HAp-ferrite hybrid particles synthesized using two-step ultrasonic spray pyrolysis.

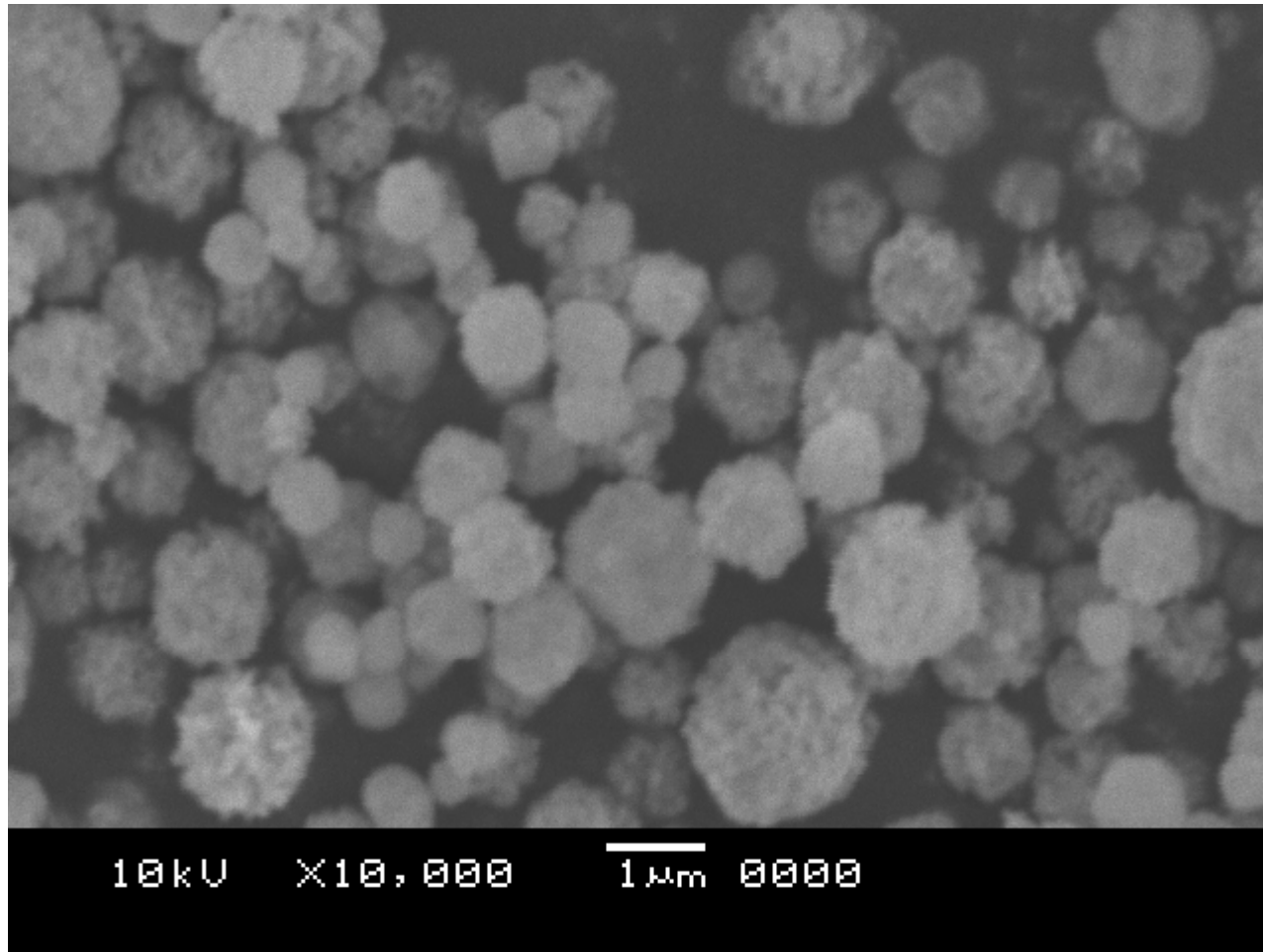


Fig. 3. SEM photograph of HAp-ferrite hybrid particles.

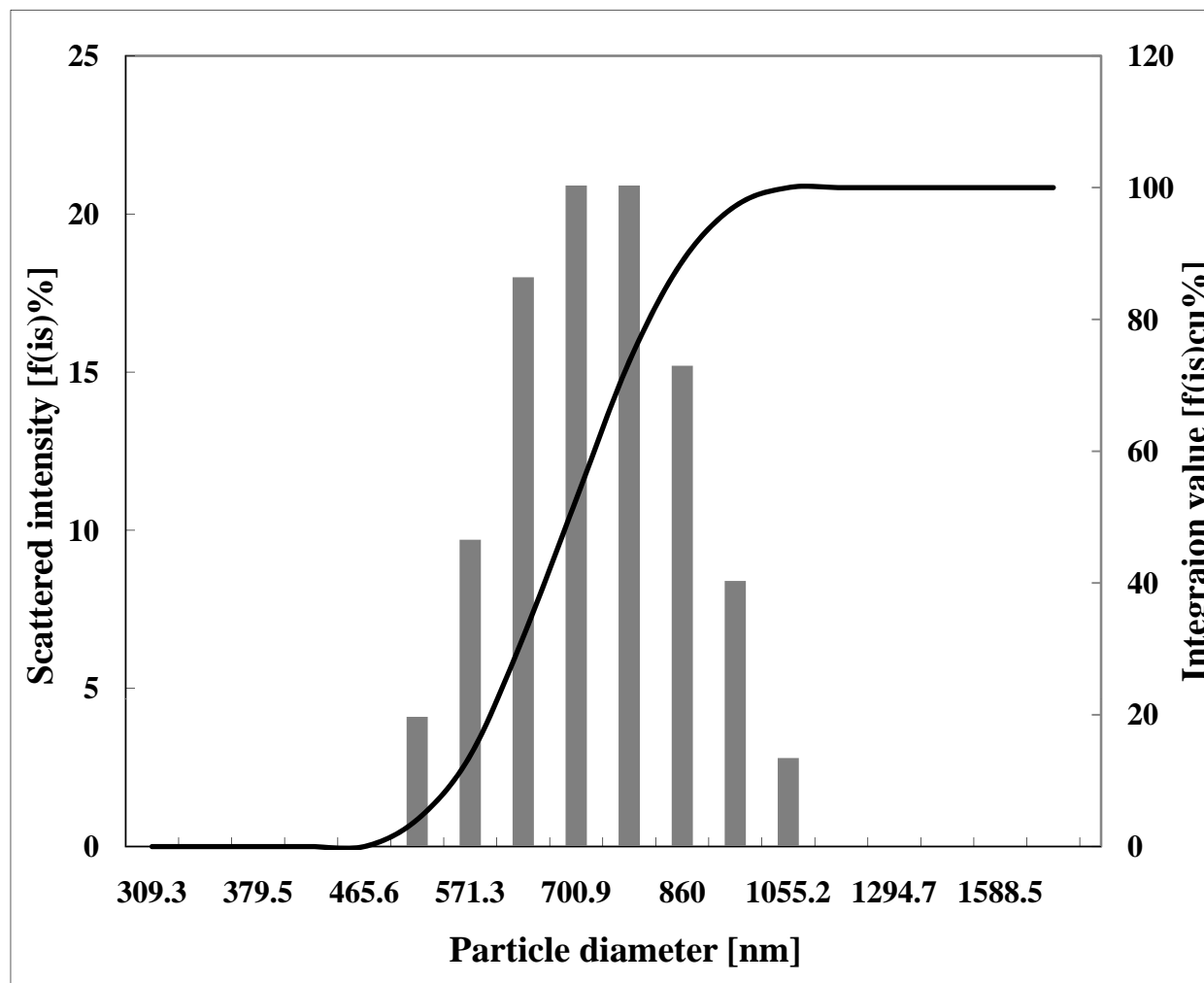


Fig. 4. Size distribution of HAp-ferrite hybrid particles obtained using the electrophoretic scattering photometer.

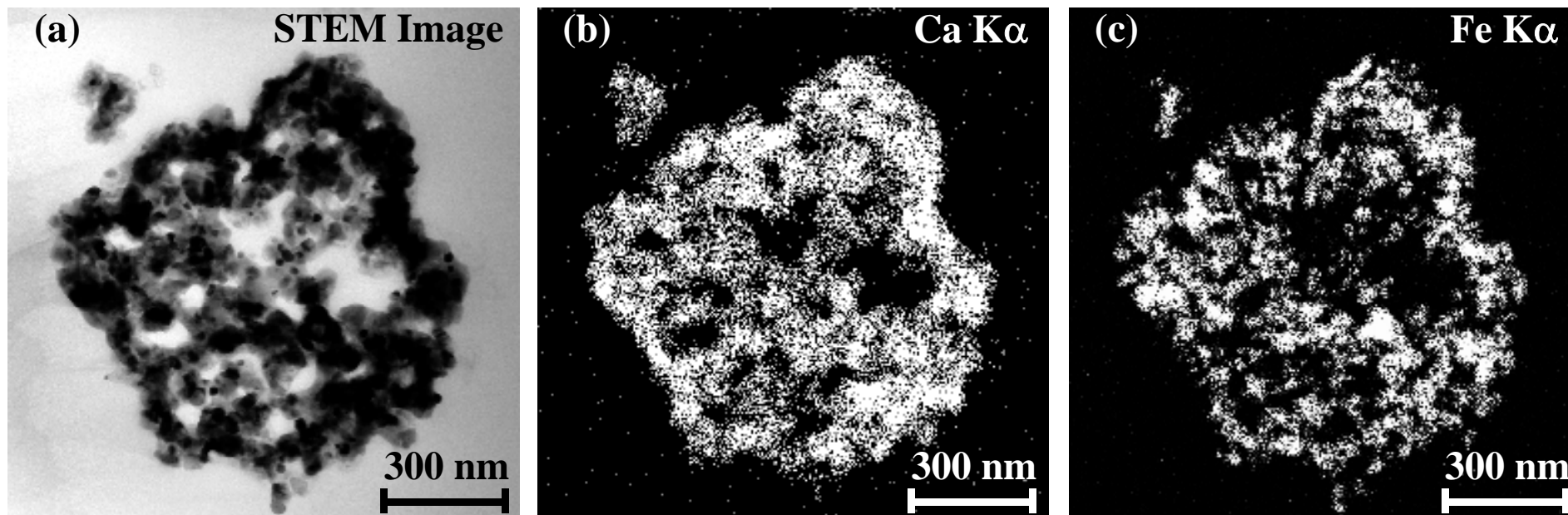


Fig. 5. STEM--EDS micrographs of the cross sectional structure of HAp-ferrite hybrid particles.

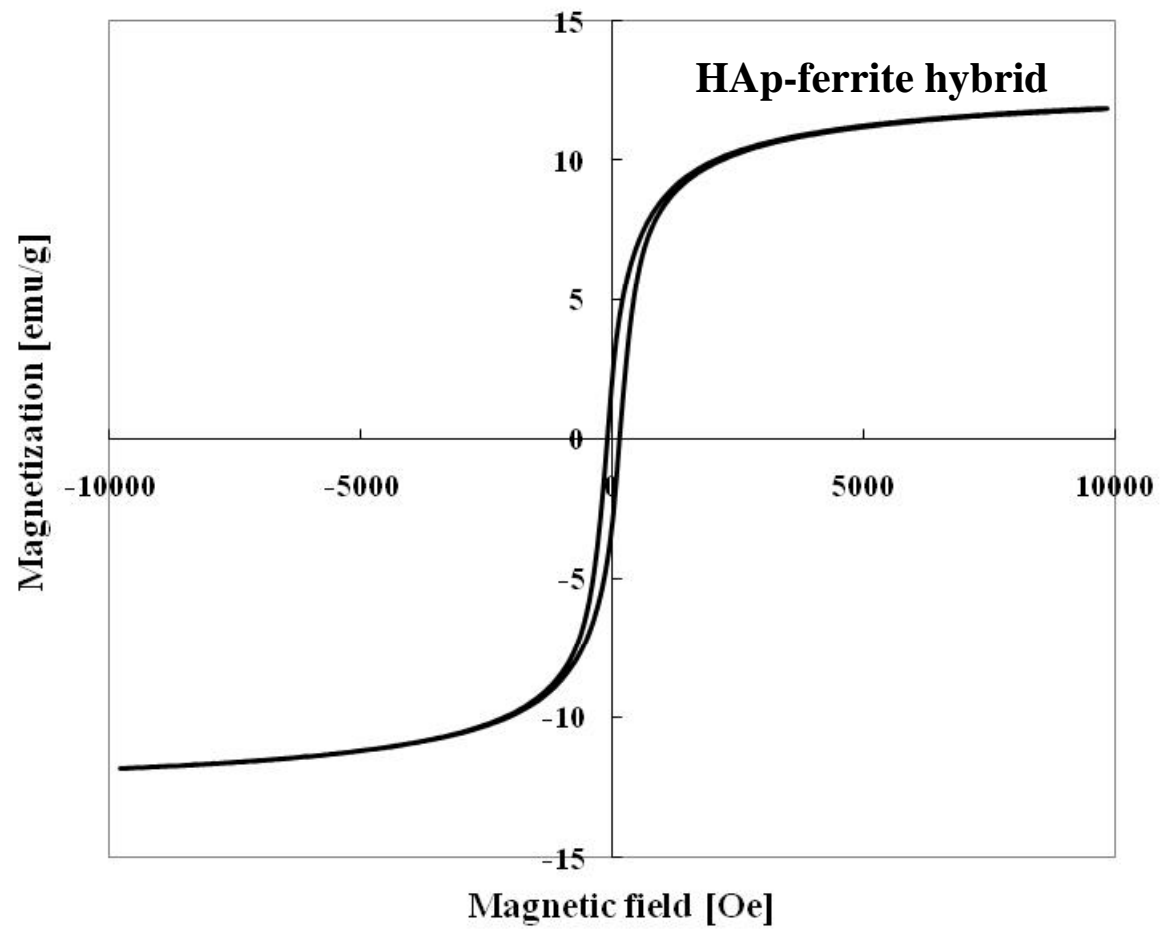


Fig. 6. M--H curve of HAp-ferrite particles synthesized using two-step ultrasonic spray pyrolysis.

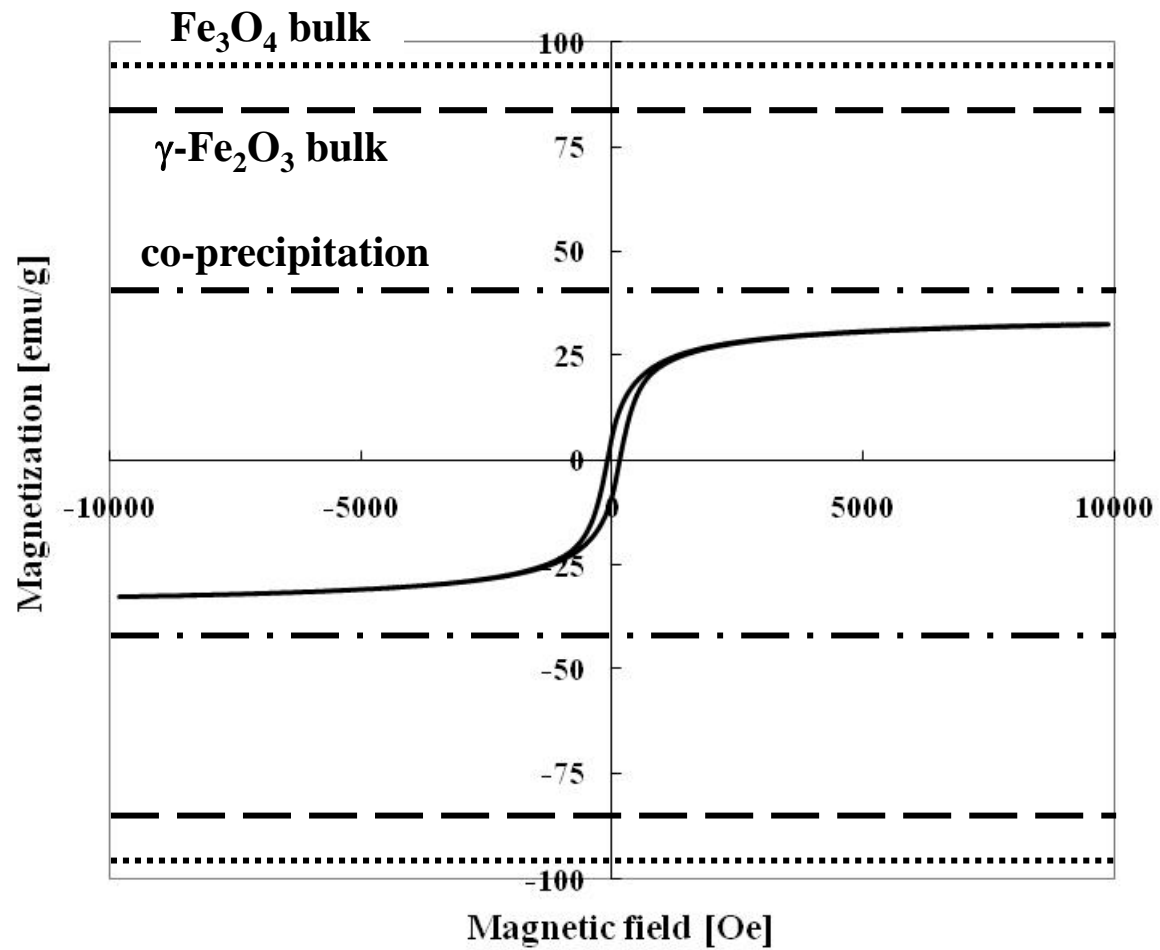


Fig. 7. M--H curve calculated based on the TOPAS result.

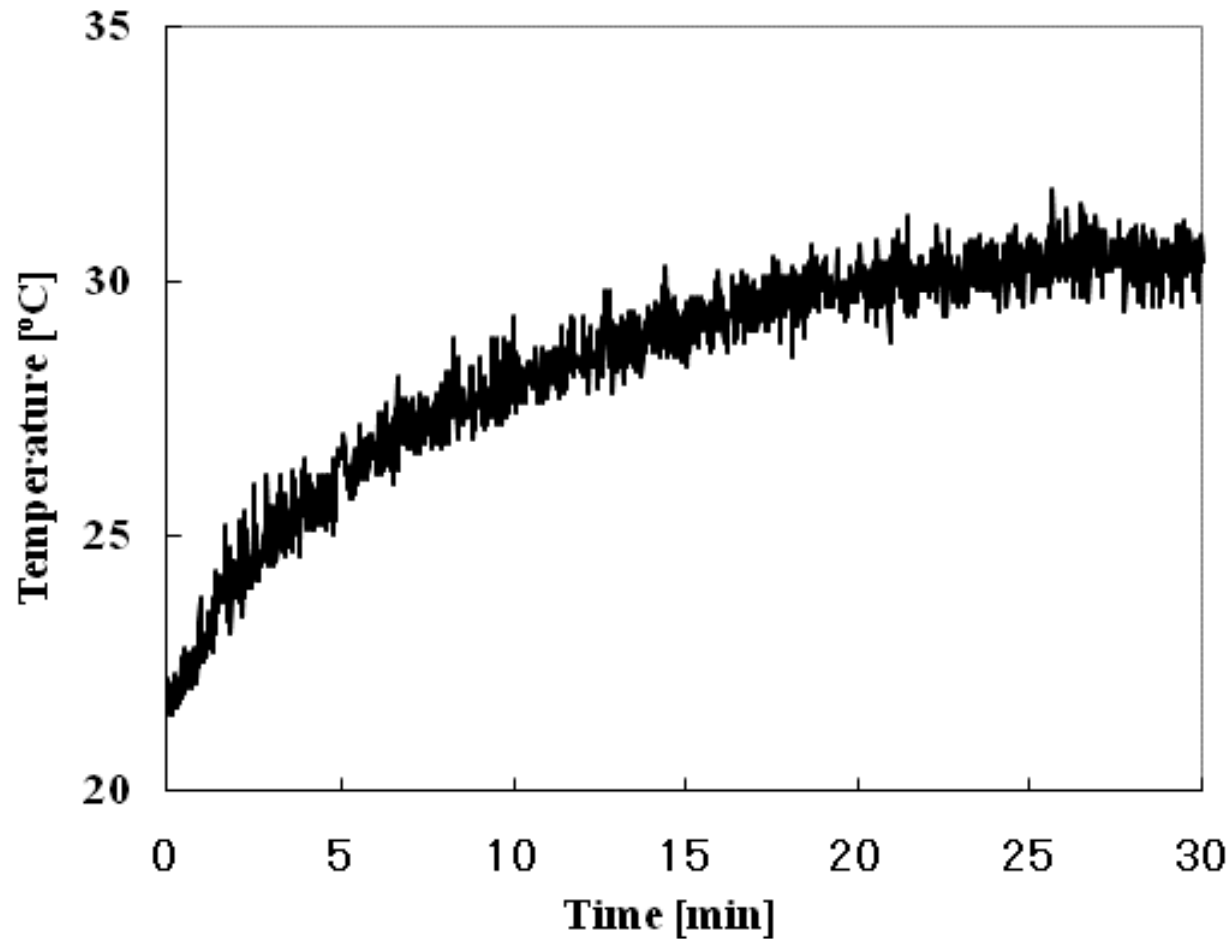


Fig. 8. Temperature for the HAp-ferrite hybrid particles synthesized by two-step ultrasonic spray pyrolysis in AC-magnetic fields (370 kHz, 1.77 kA/m).